Aerosol and Air Quality Research, 17: 2726–2734, 2017

ISSN: 1680-8584 print / 2071-1409 online
doi: 10.4209/aaqr.2016.08.0352

Preparation and Characterization of CeO_2-MoO_3/TiO_2 Catalysts for Selective Catalytic Reduction of NO with NH_3

Ye Jiang*, Xuechong Wang, Zhimin Xing, Changzhong Bao, Guitao Liang

College of Pipeline and Civil Engineering, China University of Petroleum, Qingdao 266580, China

ABSTRACT

CeO_2-MoO_3/TiO_2 catalysts were prepared by three methods: a single step sol-gel (SG), impregnation (IM) and coprecipitation (CP) method. These catalysts were investigated for selective catalytic reduction (SCR) of NO with NH_3. The results indicate that the catalyst prepared by the SG method possessed the widest temperature window (about 250–475°C), best SCR activity below 450°C and resistance against 10% H_2O and 1000 ppm SO_2 at a gas hourly space velocity (GHSV) of 90,000 h^{-1}. According to the results of BET, XRD, XPS, H_2-TPR and TEM, it is found that larger BET surface area, more highly dispersed active species of Ce and Mo, presence of more Ce^{3+} and chemisorbed oxygen, synergistic effect among ceria, molybdenum and titania, and better redox ability can contribute to the better deNO_x performance of the CeO_2-MoO_3/TiO_2 catalyst prepared by the SG method, compared with those by the IM and CP methods.

Keywords: Selective catalytic reduction (SCR); CeO_2-MoO_3/TiO_2; NO removal; NH_3; Preparation methods.

INTRODUCTION

Nitrogen oxides (NO_x), emitted from mobile and stationary sources, are to blame for the worsening environment because of their contribution to acid rain, photochemical smog, haze formation and ozone depletion. The selective catalytic reduction (SCR) with NH_3 is currently the most efficient technology for the abatement of NO_x in the flue gas from stationary sources such as coal-fired power plants and municipal solid waste (MSW) incineration plants (Busca *et al.*, 1998; Roy *et al.*, 2009). V_2O_5-WO_3(MoO_3)/TiO_2 has been put into industrial applications for the past few decades (Pârvulescu *et al.*, 1998; Fu *et al.*, 2014). However, some unavoidable issues have to be raised, such as a relatively narrow operating temperature range (300–400°C), high activity for the oxidation of SO_2 to SO_3 with increasing vanadium loadings (Dunn *et al.*, 1998), formation of N_2O at high temperatures above 400°C (Yates *et al.*, 1996) and toxicity of vanadium species.

Owing to the before-mentioned disadvantages of vanadium-based catalysts, an increasing number of researchers have recently turned their attention to ceria for the NH_3-SCR reaction due to their high oxygen storage capacity and outstanding redox property (Luo *et al.*, 2001; Guo *et al.*, 2014; Zhu *et al.*, 2015). Ceria have been reported to be mixed with other metal oxides such as TiO_2 (Xu *et al.*, 2008; Gao *et al.*, 2010a; Shan *et al.*, 2012), Al_2O_3 (Shen *et al.*, 2009, Guo *et al.*, 2013), WO_3 (Peng *et al.*, 2013), MoO_3 (Li and Li, 2014), etc. In our previous study, we developed a CeO_2-MoO_3/TiO_2 catalyst, which exhibited high SCR activity and excellent resistance against 10% H_2O and 1000 ppm SO_2 (Jiang *et al.*, 2015). It is well accepted that catalyst preparation method has a substantial impact on the loading, dispersion and interaction of the active components (Lee *et al.*, 2014). In addition, because of the presence of H_2O and SO_2 in flue gas, the resistance against them is important for any potential SCR catalysts from a practical point view. Therefore, it is indispensable to investigate the relation between preparation method and the SCR activity of CeO_2-MoO_3/TiO_2 catalysts in the absence and presence of H_2O and SO_2.

In this work, CeO_2-MoO_3/TiO_2 catalysts were prepared by three methods: a single step sol-gel (SG), impregnation (IM) and coprecipitation (CP) method. The main purpose of this investigation was to determine an optimal method for preparing CeO_2-MoO_3/TiO_2 catalysts with the best deNO_x performance.

METHODS

Catalyst Preparation

In this work, the mass ratio of CeO_2:MoO_3:TiO_2 was 2:1:10 in the prepared CeO_2-MoO_3/TiO_2 catalysts. The CeO_2-MoO_3/TiO_2 catalysts were denoted as CMT(*y*), where *y* represented the preparation method of CeO_2-MoO_3/TiO_2 catalyst. Nitric acid, anhydrous ethanol and aqueous ammonia

* Corresponding author.
Tel.: +86-532-86981767; Fax: +86-532-86981882
E-mail address: jiangye@upc.edu.cn

(3 mol L^{-1}) were purchased from Xilong Chemical Industry Corp. (Guangzhou, China), and other reagents (analytically pure) used in the catalyst preparation were purchased from Sinopharm Chemical Reagent Corp. (Shanghai, China).

Single step Sol-Gel Method (SG)

One solution of butyl titanate (0.1 mol) and anhydrous ethanol (2.3 mol) was added dropwisely to the other solution of deionized water (1.9 mol), anhydrous ethanol (0.6 mol), nitric acid (0.1 mol) and cerium nitrate (0.01 mol) at room temperature under continuous and vigorous stirring for 3 h to yield a transparent colloidal solution. The solution was dried at 80°C for 24 h to form the xerogel, and then calcined in air at 500°C for 5 h.

Impregnation Method (IM)

The catalyst was prepared by impregnation of TiO_2 (0.125 mol) with an aqueous solution containing cerium nitrate (0.012 mol) and ammonium molybdate (0.001 mol). The sample was dried at 110°C for 12 h, followed by calcination in air at 500°C for 5 h.

Coprecipitation Method (CP)

Titanium sulfate (0.125 mol), cerium nitrate (0.012 mol) and ammonium molybdate (0.001 mol) were dissolved in deionized water (11.1 mol). Aqueous ammonia was slowly added to the solution under continuous and vigorous stirring at room temperature until pH reached 11. After aged for 3 h, the sediment was filtered and washed with deionized water for six times to eliminate sulfate. The obtained sample was dried at 110°C for 12 h, and then calcined in air at 500°C for 5 h.

SCR Activity Measurements

The SCR activity measurements were carried out in a fixed-bed quartz reactor of 8 mm inner diameter using 0.35 g catalyst (150–250 μm). The feed gas composition was as follows: 1000 ppm NO, 1000 ppm NH_3, 3 vol.% O_2, 10 vol.% H_2O (when used), 1000 ppm SO_2 (when used) and N_2 as balance gas. H_2O was injected with a micro-syringe pump (Smiths Medical Instrument (Zhejiang) Corp.) into a tube preheater to generate vapor. In all the tests, the total flow rate of the feed gas was 500 mL min^{-1}, corresponding to the gas hourly space velocity (GHSV) of 90,000 h^{-1}. The experiments were performed at 150–500°C. The concentrations of NO, NO_2, SO_2 and O_2 were continuously monitored by the gas analyzer (350 Pro, Testo). The formation of N_2O was found to be negligible (< 10 ppm), and consequently this product would not be further discussed.

Characterization of Catalysts

The specific surface area, total pore volume and average pore diameter of the catalysts were measured by N_2 adsorption/desorption at –196°C using a ASAP2020-M system (Micromeritics Instrument Corp.). The specific surface area were evaluated by the Brunauer-Emmette-Teller (BET) method. The pore size distribution was measured using Barrett-Joyner-Halenda (BJH) method.

The crystallite structure was identified by the X-ray diffractometer (Panalytical Corp.) with a X′Pert PRO MPD system by using Cu Ka radiation.

X-ray photoelectron spectroscopy (XPS) was used to determine the atomic concentration and the chemical state of the elements on the catalyst surface with a Thermo ESCALAB 250 spectrometer using monochromated Al Kα X-rays (hν = 1486.6 eV) as a radiation source at 150 W. The binding energies were referenced to the C 1s line at 284.6 eV.

To evaluate the redox ability of the catalysts, temperature programmed reduction (H_2-TPR) was performed on an Autosorb-iQ-C chemisorption analyzer (Quantachrome Instrument Corp.) with a thermal conductivity detector (TCD).

The catalysts were analyzed with a JOEL JEM-2010 electron microscope to observe their microstructures.

RESULTS AND DISCUSSION

Catalytic Activity Evaluation

NH_3-SCR Activity

The activities of various samples for the SCR of NO with NH_3 were measured as a function of temperatures and the results are shown in Fig. 1. It was clear that CMT(SG) possessed the best catalytic performance at the temperature below 450°C and the widest activity temperature window (about 250–475°C) for > 90% NO conversion. When the reaction temperature exceeded 450°C, the activity was shown as follows: CMT(CP) > CMT(SG) > CMT(IM). These indicated that catalyst preparation methods had a massive impact on the SCR performance of CeO_2-MoO_3/TiO_2 catalysts.

Effect of H_2O and SO_2

H_2O and SO_2 are the main components in flue gas from stationary sources, so it is important to investigate their effect on the SCR activities of various catalysts and the results are shown in Figs. 2–4. As shown in Fig. 2, when H_2O was added into the feed gas, the activity of CMT(SG) decreased a little in the temperature range of 150–300°C and was not nearly inhibited at 300–450°C. As for CMT(IM), the presence of H_2O caused a marked decrease in its activity at the temperatures below 400°C and had almost no inhibition at 400–450°C. It was noted that NO conversions over CMT(SG) and CMT(IM) were both enhanced at 500°C after the addition of H_2O, and yet the activity of CMT(SG) was higher than that of CMT(IM). With regard to CMT(CP), a nearly complete loss of its activity was observed. The H_2O adsorbed on catalyst surface can block the active sites, leading to the decrease of the NH_3-SCR activity (Liu *et al.*, 2014b). It could be seen that CMT(SG) had the best tolerance to H_2O in these three samples.

Effect of SO_2 on NO conversion over CeO_2-MoO_3/TiO_2 catalysts prepared by different methods is shown in Fig. 3. Before adding SO_2, the SCR reaction had been stabilized for 1 h, and nearly 100% of NO conversions were achieved over CMT(SG) and CMT(IM). The addition of 1000 ppm SO_2 to the feed gas had little effect on the catalytic activities of CMT(SG). On the contrary, the catalytic activity of CMT(IM) decreased with time and about 80% NO conversion was

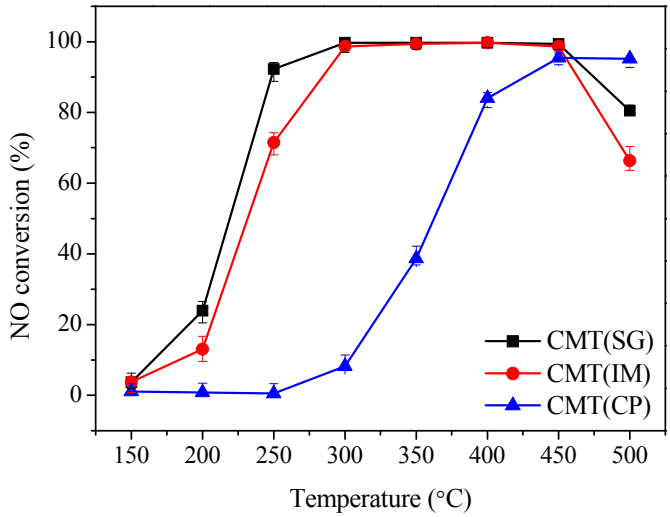

Fig. 1. NO conversion as a function of reaction temperature for various catalysts. Reaction conditions: [NO] = [NH_3] = 1000 ppm, [O_2] = 3 vol.%, balance N_2 and GHSV = 90,000 h^{-1}.

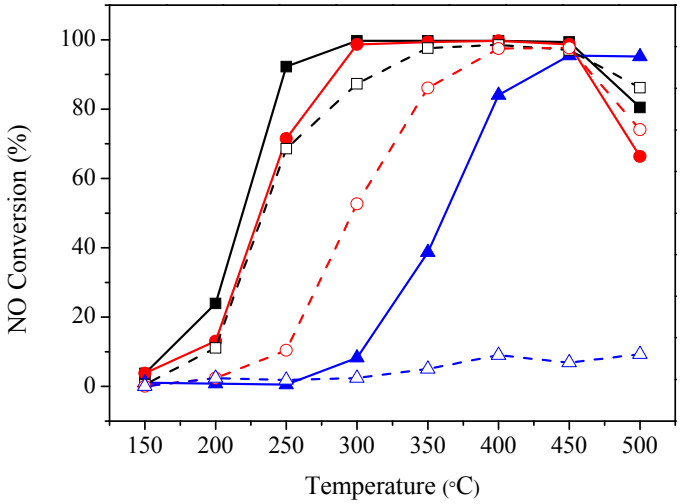

Fig. 2. Effect of H_2O on NO conversion over various catalysts. (■□) CMT(SG), (●○) CMT(IM), (▲△) CMT(CP). Reaction conditions: [NO] = [NH_3] = 1000 ppm, [O_2] = 3 vol.%, [H_2O] = 10% (□○△), balance N_2 and GHSV = 90,000 h^{-1}.

obtained after 7.5 h. As for CMT(CP), the original activity was substantially lower than those of the other two catalysts. After the addition of SO_2, it still remained the original low activity. From Fig. 3, it can be also seen that there were almost no changes in the activities of CMT(IM) and CMT(CP) when SO_2 was cut off. According to Xu *et al.* (2009), the presence of SO_2 in the feed gas led to the formation of NH_4HSO_4, $Ce(SO_4)_2$ and $Ce_2(SO_4)_3$ on Ce/TiO_2 catalyst. NH_4HSO_4 could deposit on the surface of the catalyst and block the active sites. $Ce(SO_4)_2$ and $Ce_2(SO_4)_3$ disrupted the Ce^{3+}/Ce^{4+} redox cycle and inhibited the formation and adsorption of nitrate species (Xu *et al.*, 2009). Compared with CMT(IM) and CMT(CP), CMT(SG) might inhibit the formation of these surface sulfate species, thereby having the best tolerance to SO_2.

Fig. 4 illustrates the co-effect of H_2O and SO_2 on NO conversion over various catalysts. CMT(SG) exhibited the highest resistance to H_2O and SO_2 and a relatively high NO conversion (about 80%) was still maintained after 7.5 h. Upon switching off H_2O and SO_2, the activity was nearly restored to its original level. For CMT(IM), the NO conversion decreased sharply to about 10% in 3.5 h and subsequently the low activity was retained. As to CMT(CP), the addition of H_2O and SO_2 led to the rapid decrease in its activity and less than 10% of NO conversion was obtained after 3.5 h. After removing H_2O and SO_2, only a very small part of the SCR activity was restored over CMT(IM) and CMT(CP). It was obvious that the preparation methods had a different impact on the resistance of CeO_2-MoO_3/TiO_2 catalysts to H_2O and SO_2. It is known that $Ce(SO_4)_2$ and $Ce_2(SO_4)_3$ have high thermal stability (Xu *et al.*, 2009). Considering that the removal of H_2O and SO_2 resulted in regaining the activity of CMT(SG), the deactivation of CMT(SG) by H_2O and SO_2 might be mainly attributed to the deposition of NH_4HSO_4, blocking the active sites on the catalyst surface. Furthermore, SO_2 hardly reacted with

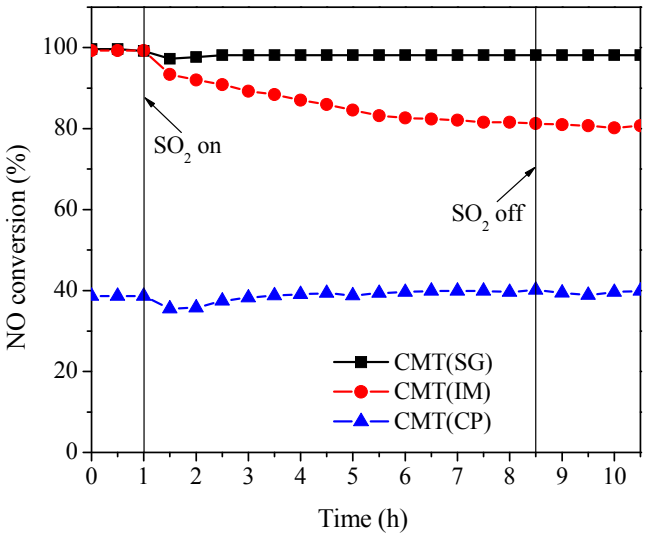

Fig. 3. Effect of SO_2 on NO conversion over various catalysts at 350°C. Reaction conditions: [NO] = [NH_3] = 1000 ppm, [O_2] = 3 vol.%, [SO_2] = 1000 ppm, balance N_2 and GHSV = 90,000 h^{-1}.

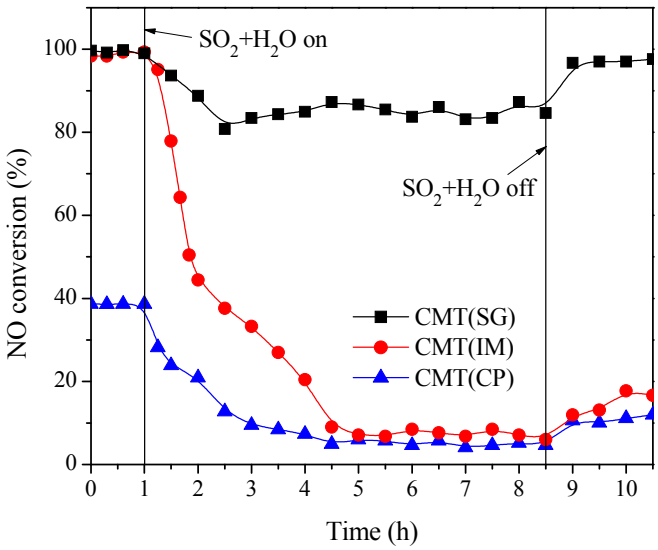

Fig. 4. Effect of H_2O and SO_2 on NO conversion over various catalysts at 350°C. Reaction conditions: [NO] = [NH_3] = 1000 ppm, [O_2] = 3 vol.%, [H_2O] = 10%, [SO_2] = 1000 ppm, balance N_2 and GHSV = 90,000 h^{-1}.

CMT(SG) to form $Ce(SO_4)_2$ and $Ce_2(SO_4)_3$. It might be ascribed to the competitive adsorption of H_2O at the catalyst surface and the strong interaction among Ce, Mo and Ti in CMT(SG). By contrast, the great loss of the activity of CMT(IM) and CMT(CP) might be attributed to the formation of NH_4HSO_4, $Ce(SO_4)_2$ and $Ce_2(SO_4)_3$.

Characterization of Catalysts

BET Results

The physical properties of the CeO_2-MoO_3/TiO_2 catalysts prepared by different methods are compared in Table 1. The BET surface area of CMT(SG) was the largest among the three samples. The total pore volume is in the following sequence: CMT(SG) < CMT(IM) < CMT(CP). The order of the average pore diameter was: CMT(SG) < CMT(CP) < CMT(IM). It was clear that different preparation methods could result in the different microstructure of CeO_2-MoO_3/TiO_2 catalysts. The similar phenomena were found over CeO_2/TiO_2 (Gao *et al.*, 2010b), CeO_2/Al_2O_3 (Guo *et al.*, 2013) and CeO_2-ZrO_2-WO_3 (Ning *et al.*, 2015) prepared by different methods.

XRD Results

XRD patterns of various samples are presented in Fig. 5. CMT(SG) exhibited only the characteristic lines of anatase TiO_2. The absence of the characteristic diffraction peaks due to CeO_2 and MoO_3 indicated that CeO_2 and MoO_3 were highly dispersed and existed as amorphous or highly dispersed species on the surface of anatase TiO_2. This also suggested that there existed a strong synergistic effect among Ce, Mo and Ti in CMT(SG). By contrast, an extremely weak diffraction peak of $Ce_2(MoO_4)_3$ (PDF30-0303) was

Table 1. Physical properties of different samples.

Samples	BET surface area (m^2 g^{-1})	Total pore volume (cm^3 g^{-1})	Average pore diameter (nm)
CMT(IM)	65.30	0.2464	12.749
CMT(SG)	103.90	0.1779	5.664
CMT(CP)	101.53	0.3480	11.882

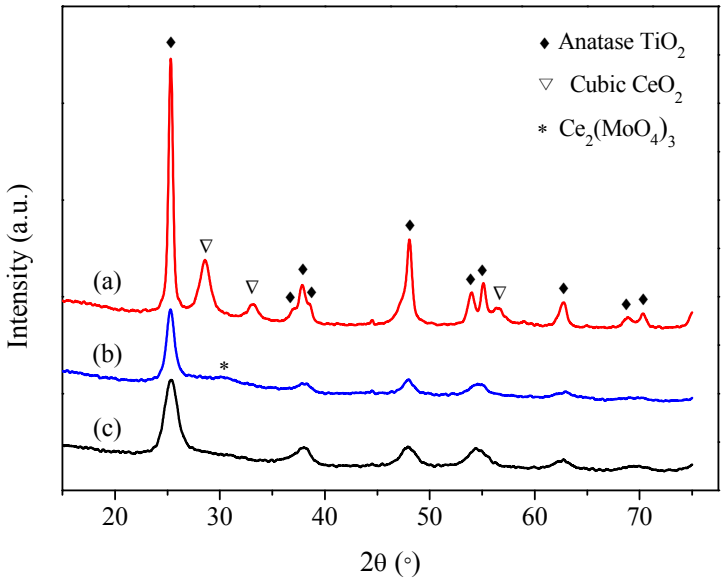

Fig. 5. XRD patterns of (a) CMT(IM), (b) CMT(CP) and (c) CMT(SG).

observed on CMT(CP) in addition to the characteristic lines of anatase TiO_2. As for CMT(IM), quite a few diffraction peaks ascribed to cubic CeO_2 were detected, as reported by Liu *et al.* (2014a). This implied that ceria crystallites were present in CMT(IM). Furthermore, it can be seen from Fig. 5 that the sharpness and relative intensity of the main anatase peak (101) for CMT(IM) was obviously larger than the two other samples. This indicated the interaction was weakest among Ce, Mo and Ti in CMT(IM), thereby giving rise to the segregation of CeO_2 crystallites from TiO_2 carrier. It seems reasonable to suppose that, over the CeO_2-MoO_3/TiO_2 catalyst prepared by a single step sol-gel method, ceria could be well dispersed and kept as an amorphous phase, which would help to improve its catalytic activity.

XPS Results

Complicated XPS spectra of Ce 3d for various samples are illustrated in Fig. 6. The sub-bands labeled u, u″, u‴ and v, v″, v‴ are assigned to Ce^{4+}, while u′ and v′ belong to Ce^{3+} (Gao *et al.*, 2010c; Chen *et al.*, 2010; Shan *et al.*, 2012). It is generally acknowledged that ceria-based catalysts possess the excellent reducibility via the redox shift between Ce^{3+} and Ce^{4+}, which enhances the oxygen store/release capacity. Accordingly, the SCR activity of CeO_2-MoO_3/TiO_2 catalyst should have something to do with the ratio of $Ce^{3+}/(Ce^{3+}+Ce^{4+})$. From Fig. 6, it can be seen that the redox couple of Ce^{3+}/Ce^{4+} was observed in all of the three samples. The ratios of $Ce^{3+}/(Ce^{3+}+Ce^{4+})$ for CeO_2-MoO_3/TiO_2 catalysts were shown as follows: 26.3% for CMT(IM) < 35.4% for CMT(CP) < 41.7% for CMT(SG). This indicated that preparation methods could lead to the difference in the Ce valance state over CeO_2-MoO_3/TiO_2 catalysts while more Ce^{3+} were present in CMT(SG). The existence of Ce^{3+} could create a charge imbalance, vacancies and unsaturated chemical bonds on the catalyst surface, leading to the increase in chemisorbed oxygen or/and weakly bonded oxygen species on the catalyst surface (Yang *et al.*, 2006). As a result, it could be inferred that CMT(SG) would possess superior deNO_x performance, which had been exactly confirmed by the results of the activity tests.

The O 1s XPS spectra of various samples can be fitted into three overlapping peaks, as shown in Fig. 7. The sub-band at 529.0–530.1 eV can be assigned to the lattice oxygen (denoted by O_α) (Chen *et al.*, 2010; Gao *et al.*, 2010c). Two shoulder peaks at 530.6–531.0 eV and 532.4–533.0 eV are ascribed to the surface adsorbed oxygen (denoted by O_β) and the surface oxygen by hydroxyl species and/or adsorbed water species as contaminants at the surface (denoted by O_γ), respectively (Yang *et al.*, 2006; Chen *et al.*, 2010; Gao *et al.*, 2010c). The calculated O_β ratio increased according to the following sequence: 31.2% for CMT(IM) < 32.7% for CMT(CP) < 34.1% for CMT(SG). Surface adsorbed oxygen (O_β) has been reported to play a substantial role in SCR reaction due to its higher mobility than lattice oxygen (O_α) (Shan *et al.*, 2012). High O_β ratio facilitated the oxidation of NO to NO_2 in the SCR reaction (Adamowska *et al.*, 2008; Chen *et al.*, 2012), thereby improving the activity of the catalysts. This was in good agreement with the results of the activity tests.

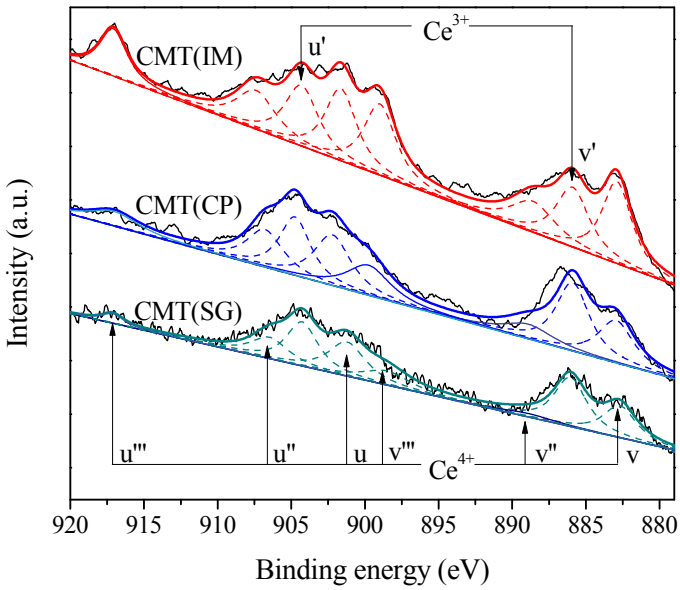

Fig. 6. XPS spectra of Ce 3d for various catalysts.

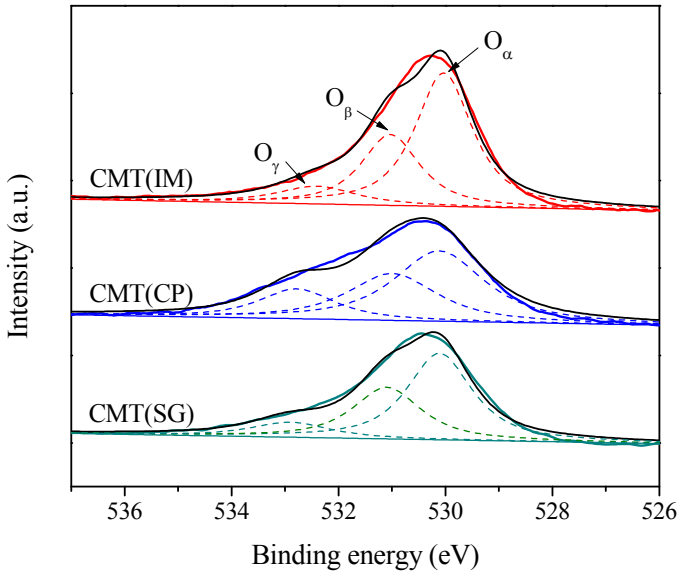

Fig. 7. XPS spectra of O 1s for various catalysts.

H_2-TPR Results

H_2-TPR profiles of various samples are compared in Fig. 8. For CMT(SG), a single broad reduction peak centered at 548°C was observed and the onset temperature (T_{onset}) was about 350°C. The reduction process of CMT(SG) could be interpreted as the coreduction of surface oxygen of ceria and well dispersed Mo species. It should be noted that the reduction of bulk ceria did not take place in the temperature range of 300−700°C, since it occurred only above 750°C (Devaiah *et al.*, 2014; Li *et al.*, 2014). CMT(IM) possessed two reduction peaks entered at 478°C and 747°C, which was similar to that reported in the study of Liu *et al.* (2014a). The first peak could be associated with the coreduction of surface oxygen of ceria and octahedral well dispersed Mo species, while the second peak could be assigned to the coreduction of bulk ceria and tetrahedral Mo species (Liu *et al.*, 2014a). As for CMT(CP), the reduction temperature of the main peak shifted to higher temperature (612°C). From Fig. 8, it could be also found that T_{onset} of CMT(SG) was the lowest among the three samples. This suggested that CMT(SG) could be reduced most easily. From the BET and XRD results, it could be inferred that the easier reduction for CMT(SG) might be attributed to its higher surface area and better dispersion of Ce and Mo on TiO_2 carrier, which were highly beneficial in improving the activity of the catalysts. In addition, it should be noted that CMT(SG) and CMT(CP) showed distinct H_2-TPR behaviors though displayed similar crystallinity of anatase TiO_2 and dispersion of ceria and MoO_3 (Fig. 5). This implied that the interaction among Ce, Mo and Ti might have a significant impact on

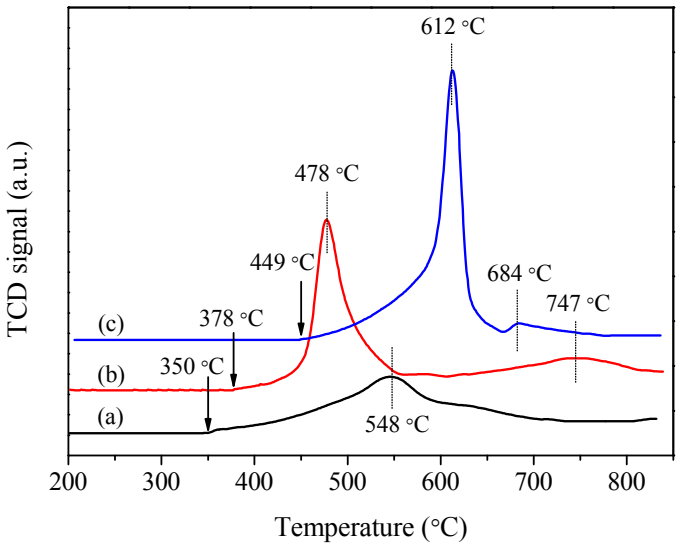

Fig. 8. H_2-TPR profiles of (a) CMT(SG), (b) CMT(IM) and (c) CMT(CP).

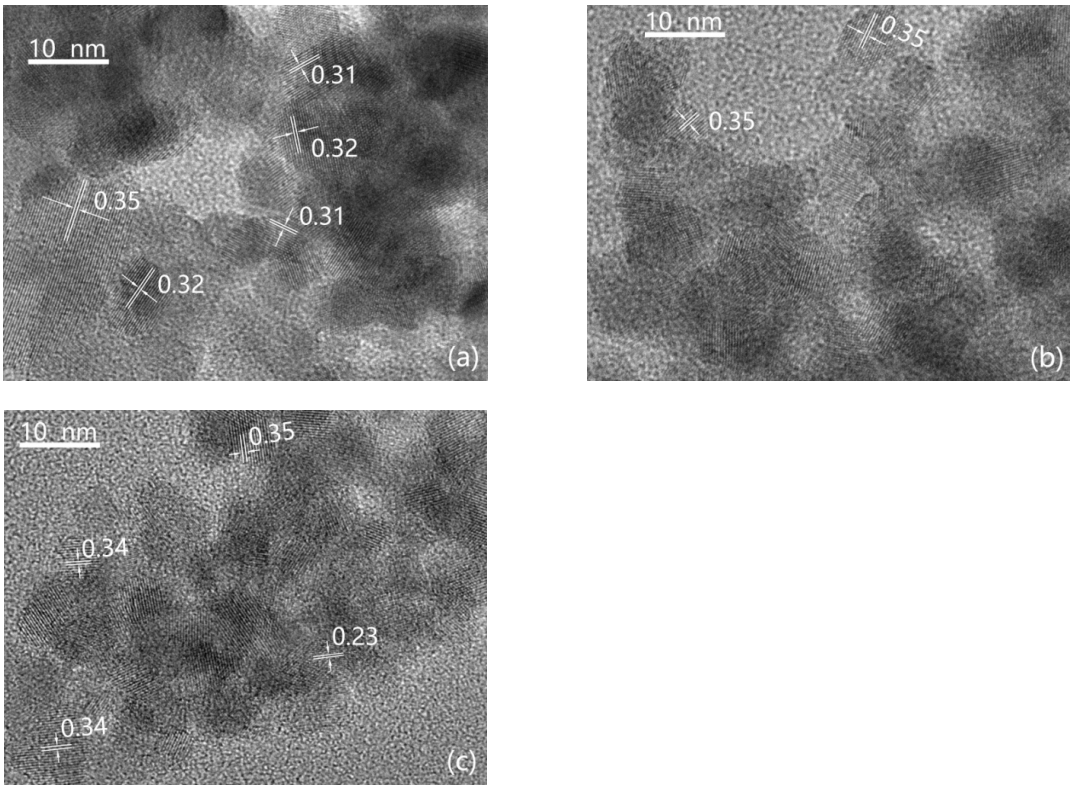

Fig. 9. TEM micrographs of (a) CMT(IM), (b) CMT(SG) and (c) CMT(CP).

the reducibility of the samples. According to the XPS results, the ratios of Ce^{3+}/Ce^{4+} were different in various samples. It has been reported that Mo^{6+} species can be present in both tetrahedral and octahedral coordination (Park *et al.*, 1997). Therefore, it can be inferred that the difference in H_2 consumption for various samples was likely to correlate with the formation of subtly different surface structure of Ce and Mo oxide species, resulting from different catalyst preparation methods. H_2-TPR results demonstrated that CMT(SG) possessed the excellent redox ability.

TEM Results

The HR-TEM micrographs of various samples are shown in Fig. 9. As shown in Fig. 9(a), the primary particle size of CMT(IM) was about 20 nm, and the crystals of TiO_2 and CeO_2 could be observed distinctly. This implied that crystalline phase of TiO_2 and CeO_2 existed in CMT(IM), which was consistent with XRD results. There were three kinds of lattice fringes. 0.35 nm, 0.32 nm and 0.31 nm of lattice fringes matched anatase (101) (Jiang *et al.*, 2015), CeO_2 (111) (Vantomme *et al.*, 2005) and MoO_3 (021) (Jiang

and Song, 2007), respectively. It was noted that MoO_3 was not determined by XRD. It might be because MoO_3 was well dispersed and existed as amorphous or highly dispersed species in CMT(IM). For CMT(SG) and CMT(CP), the primary particle size was less than 10 nm, and the crystals of TiO_2, CeO_2 and MoO_3 could be not discriminated. These results indicated that less crystalline phase of TiO_2 formed in these two samples, which was in good agreement with XRD results. In CMT(SG), only lattice fringes ascribed to anatase TiO_2 were determined. This meant that CeO_2 and MoO_3 were well dispersed and existed as amorphous or highly dispersed species. As to CMT(CP), besides the lattice fringes matching anatase (101), 0.34 nm and 0.23 nm of lattice fringes were identified, which were ascribed to MoO_3 (040) (Du *et al.*, 2014) and MoO_3 (041) (Zhong *et al.*, 2014). According to the XRD results, $Ce_2(MoO_4)_3$ was present in CMT(CP). Therefore, it could be concluded that a single step sol-gel method might improve the dispersion of CeO_2 and MoO_3 in CMT(SG), which was conducive to enhance its catalytic activity.

CONCLUSIONS

CeO_2-MoO_3/TiO_2 catalysts were prepared by three methods. The catalyst prepared by a single step sol-gel method showed the best SCR activity and resistance to 10% H_2O and 1000 ppm SO_2. From the results of BET, XRD, XPS, H_2-TPR and TEM, it could be inferred that the superior deNO_x performance should be attributed to large surface area, highly dispersed active species of Ce and Mo, presence of more Ce^{3+} and chemisorbed oxygen, strong interaction among ceria, molybdenum and titania, and good redox ability. As a result, a single step sol-gel method is an effective one for the preparation of CeO_2-MoO_3/TiO_2 catalyst for NH_3-SCR of NO.

ACKNOWLEDGMENTS

The authors wish to express their sincere appreciation for the financial supports from the National Science Foundation of China (No. 51506226), Shandong Provincial Natural Science Foundation (No. ZR2015EM010) and "the Fundamental Research Funds for the Central Universities" (No. 15CX05005A).

REFERENCES

Adamowska, M., Krztoń, A., Najbar, M., Costa, P.D. and Djéga-Mariadassou, G. (2008). DRIFT study of the interaction of NO and O_2 with the surface of $Ce_{0.62}Zr_{0.38}O_2$ as deNO*x* catalyst. *Catal. Today* 137: 288–291.

Busca, G., Lietti, L., Ramis, G. and Berti, F. (1998). Chemical and mechanistic aspects of the selective catalytic reduction of NO_x by ammonia over oxide catalysts: A review. *Appl. Catal. B* 18: 1–36.

Chen, L., Li, J., Ge, M. and Zhu, R. (2010). Enhanced activity of tungsten modified CeO_2/TiO_2 for selective catalytic reduction of NO_x with ammonia. *Catal. Today* 153: 77–83.

Chen, L., Weng, D., Si, Z. and Wu, X. (2012). Synergistic effect between ceria and tungsten oxide on WO_3-CeO_2-TiO_2 catalysts for NH_3-SCR reaction. *Prog. Nat. Sci.* 22: 265–272.

Devaiah, D., Jampaiah, D., Saikia, P. and Reddy B.M. (2014). Structure dependent catalytic activity of $Ce_{0.8}Tb_{0.2}O_{2-\delta}$ and TiO_2 supported $Ce_{0.8}Tb_{0.2}O_{2-\delta}$ solid solutions for CO oxidation. *J. Ind. Eng. Chem.* 20: 444–453.

Du, Y.C., Zheng, G.W., Meng, Q., Wang, L.P., Fan, H.G. and Dai, H.X. (2014). Fabrication and excellent catalytic performance of three-dimensional ordered mesoporous molybdenum oxides. *J. Inorg. Mater.* 29: 124–130 (in Chinese).

Dunn, J.P., Koppula, P.R., Stenger, H.G. and Wachs I.E. (1998). Oxidation of sulfur dioxide to sulfur trioxide over supported vanadia catalysts. *Appl. Catal. B* 19: 103–117.

Fu, M., Li, C., Lu, P., Qu, L., Zhang, M., Zhou, Y., Yu, M. and Fang, Y. (2014). A review on selective catalytic reduction of NO_x by supported catalysts at 100-300°C–catalysts, mechanism, kinetics. *Catal. Sci. Technol.* 4: 14–25.

Gao, X., Du, X., Cui, L., Fu, Y., Luo, Z. and Cen, K. (2010a). A Ce-Cu-Ti oxide catalyst for the selective catalytic reduction of NO with NH_3. *Catal. Commun.* 12: 255–258.

Gao, X., Jiang, Y., Fu, Y., Zhong, Y., Luo, Z. and Cen, K. (2010b). Preparation and characterization of CeO_2/TiO_2 catalysts for selective catalytic reduction of NO with NH_3. *Catal. Commun.* 11: 465–469.

Gao, X., Jiang, Y., Zhong, Y., Luo, Z. and Cen, K. (2010c). The activity and characterization of CeO_2-TiO_2 catalysts prepared by the sol-gel method for selective catalytic reduction of NO with NH_3. *J. Hazard. Mater.* 174: 734–739.

Guo, R., Zhou, Y., Pan, W., Hong, J., Zheng, W., Jin, Q., Ding, C. and Guo, S. (2013). Effect of preparation methods on the performance of CeO_2/Al_2O_3 catalysts for selective catalytic reduction of NO with NH_3. *J. Ind. Eng. Chem.* 19: 2022–2025.

Guo, R., Zhen, W., Pan, W., Zhou, Y., Hong, J., Xu, H., Jin, Q., Ding, C. and Guo S. (2014). Effect of Cu doping on the SCR activity of CeO_2 catalyst prepared by citric acid method. *J. Ind. Eng. Chem.* 20: 1577–1580.

Jiang, Y., Xing, Z., Wang, X., Huang, S., Liu, Q. and Yang, J. (2015). MoO_3 modified CeO_2/TiO_2 catalyst prepared by a single step sol-gel method for selective catalytic reduction of NO with NH_3. *J. Ind. Eng. Chem.* 29: 43–47.

Jiang, Y., Xing, Z., Wang, X., Huang, S., Wang, X. and Liu, Q. (2015). Activity and characterization of a Ce-W-Ti oxide catalyst prepared by a single step sol-gel method for selective catalytic reduction of NO with NH_3. *Fuel* 151: 124–129.

Lee, D.W. and Yoo, B.R. (2014). Advanced metal oxide (supported) catalysts: Synthesis and applications. *J. Ind. Eng. Chem.* 20: 3947–3959.

Lee, S.M., Park, K.H. and Hong, S.C. (2012). MnO_x/CeO_2-TiO_2 mixed oxide catalysts for the selective catalytic reduction of NO with NH_3 at low temperature. *Chem.*

Eng. J. 195–196: 323–331.

Li, X. and Li, Y. (2014). Selective catalytic reduction of NO with NH_3 over Ce-Mo-O_x catalyst. *Catal. Lett.* 114: 165–171.

Liu, Z., Zhang, S., Li, J. and Ma, L. (2014a). Promoting effect of MoO_3 on the NO*x* reduction by NH_3 over CeO_2/TiO_2 catalyst studied with in situ DRIFTS. *Appl. Catal. B* 144: 90–95.

Liu, Z., Zhu, J., Zhang, S., Ma, L. and Woo, S.I. (2014b). Selective catalytic reduction of NO_x by NH_3 over MoO_3-promoted CeO_2/TiO_2 catalyst. *Catal. Commun.* 46: 90–93.

Luo, M., Chen, J., Chen, L., Lu, J., Feng, Z. and Li, C. (2001). Structure and redox properties of $Ce_xTi_{1-x}O_2$ solid solution. *Chem. Mater.* 13: 197–202.

Ning, P., Song, Z., Li, H., Zhang, Q., Liu, X., Zhang, J., Tang, X. and Huang, Z. (2015). Selective catalytic reduction of NO with NH_3 over CeO_2-ZrO_2-WO_3 catalysts prepared by different methods. *Appl. Surf. Sci.* 332: 130–137.

Park, J.C. and Song, H. (2007). Synthesis of polycrystalline Mo/MoO_x nanoflakes and their transformation to MoO_3 and MoS_2 nanoparticles. *Chem. Mater.* 19: 2706–2708.

Park, Y.C., Oh, E.S. and Rhee, H.K. (1997). Characterization and catalytic activity of WNiMo/Al_2O_3 catalyst for hydrodenitrogenation of pyridine. *Ind. Eng. Chem. Res.* 36: 5083–5089.

Pârvulescu, V.I., Grange, P. and Delmon, B. (1998). Catalytic removal of NO. *Catal. Today* 46: 233–316.

Roy, S., Hegde, M.S. and Madras, G. (2009). Catalysis for NO_x abatement. *Appl. Energy* 86: 2283–2297.

Shan, W., Liu, F., Hong, H., Shi, X. and Zhang, C. (2011). The remarkable improvement of a Ce-Ti based catalyst for NO_x abatement, prepared by a homogeneous precipitation method. *ChemCatChem* 3: 1286–1289.

Shan, W., Liu, F., He, H., Shi, X. and Zhang, C. (2012). A superior Ce-W-Ti mixed oxide catalyst for the selective catalytic reduction of NO_x with NH_3. *Appl. Catal. B* 115–116: 100–106.

Shu, Y., Song, H., Quan, X. and Chen, S. (2012). Enhancement of catalytic activity over the iron-modified Ce/TiO_2 catalyst for selective catalytic reduction of NO_x with Aammonia. *J. Phys. Chem. C* 116: 25319–25327.

Vantomme, A., Yuan, Z.Y., Du, G. and Su, B.L. (2005). Surfactant-assisted large-scale preparation of crystalline CeO_2 nanorods. *Langmuir* 21: 1132–1135.

Xu, W., Yu, Y., Zhang, C. and Hong, H. (2008). Selective catalytic reduction of NO by NH_3 over a Ce/TiO_2 catalyst. *Catal. Commun.* 9: 1453–1457.

Xu, W., Hong, H. and Yu, Y. (2009). Deactivation of a Ce/TiO_2 catalyst by SO_2 in the selective catalytic reduction of NO by NH_3. *J. Phys. Chem. C* 113: 4426–4432.

Yang. S., Zhu. W., Jiang. Z., Chen, Z. and Wang, J. (2006). The surface properties and the activities in catalytic wet air oxidation over CeO_2-TiO_2 catalysts. *Appl. Surf. Sci.* 252: 8499–8505.

Yates, M., Martín, J.A., Martín-Luengo, M.Á., Suárez, S. and Blanco, J. (1996). N_2O formation in the ammonia oxidation and in the SCR process with V_2O_5-WO_3 catalysts. *Catal. Today* 107–108: 120–125.

Zhong, M., Wei, Z., Meng, X., Wu, F. and Li, J. (1996). From MoS_2 microspheres to α-MoO_3 manoplates: Growth mechanism and photocatalytic activities. *Eur. J. Inorg. Chem.* 20: 3245–3251.

Zhu, X., Gao, X., Qin, R. Zeng, Y., Qu, R., Zheng, C. and Tu, X. (2015). Plasma-catalytic removal of formaldehyde over Cu-Ce catalysts in a dielectric barrier discharge reactor. *Appl. Catal. B* 170–171: 293–300.

Received for review, August 30, 2016
Revised, January 1, 2017
Accepted, January 5, 2017